Supplementary Materials

Text S1. Adsorption Kinetics and Isotherm

The pseudo-first-order [S1] and pseudo-second-order kinetic models were used to describe the adsorption behaviors of Cu(II) [S2]:

$$\log(q_{e,exp} - q_t) = \log(q_{e,cal}) - K_1 t \quad (S1)$$

$$\frac{t}{q_t} = \frac{1}{K_2 q_{e,cal}^2} + \frac{1}{q_{e,cal}} t \quad (S2)$$

where $q_{e,exp}$ (mg/g) and q_t (mg/g) are the adsorption amount of Cu(II) by AL-PEI-CS_2 at equilibrium and time t (min), respectively; K_1 (1/min) and K_2 (g/(mg·min)) are the rate constants. In order to study the rate-controlling step, the Weber and Morris intra-particle diffusion model was introduced to analyze the kinetics data [S3]:

$$q_t = K_{id} t^{1/2} + I \quad (S3)$$

where q_t (mg/g) is the amount of Cu(II) adsorbed at any time t; K_{id} (mg/(g·$min^{1/2}$)) is rate constant of the model; I (mg/g) is the intercept and related to the thickness of boundary layer from the plots of q_t against $t^{1/2}$.

To further ascertain the real control step related to the adsorption process of Cu(II). The experimental data were calculated through the Boyd's film-diffusion model, which assumed that the boundary layer surrounded AL-PEI-CS_2 is the primary resistance to diffusion [S4] The relevant expression [S4] was given in the following:

$$F(t) = 1 - \left(\frac{6}{\pi^2}\right) \sum_{n=1}^{\infty} \left(\frac{1}{n^2}\right) \exp(-n^2 B t) \quad (S4)$$

where, F(t) = q_t/q_e is the fraction of Cu(II) adsorbed at time t and equilibrium time. B_t is a function of F(t). If F(t) values is higher than 0.85:

$$B_t = 0.4977 - \ln(1 - F(t)) \quad \text{(S5)}$$

If $F(t)$ values is lower than 0.85:

$$B_t = \left(\sqrt{\pi} - \sqrt{\pi - (\frac{\pi^2 F(t)}{3})} \right)^2 \quad \text{(S6)}$$

The Langmuir [S5] and Freundlich [S6] models were used to study adsorption isotherms, as showed in Eq.(S7) and Eq.(S8), respectively:

$$\frac{1}{q_e} = \frac{1}{q_m} + (\frac{1}{q_m K_L}) \frac{1}{C_e} \quad \text{(S7)}$$

$$\log q_e = \log K_F + \frac{1}{n} \log C_e \quad \text{(S8)}$$

where Ce (mg/L)is the residual concentration of Cu(II) at equilibrium; q_e (mg/g) is the adsorption amount of Cu(II) on per unit mass of AL-PEI-CS_2; q_m (mg/g) is maximum adsorption capacity; K_L (L/mg) is Langmuir constant; K_F (mg/($L^{(1-1/n)}$·g)) and n are constants of the Freundlich model, which respectively stand for adsorption capacity and intensity.

Pseudo-first-order and pseudo-second-order kinetic models were used to describe the data from experiments (Fig. 4(a)), in which the fitted results were given in Fig. S4(a), Fig. S4(b) and Table S1, respectively. According to Table S1, it was found that the pseudo-second-order kinetic model fitted the data well as values of correlation coefficient (R^2) are higher. These results demonstrated that the uptake of Cu(II) by AL-PEI-CS_2 was chemisorption, containing valency forces *via* sharing or exchanging electron between AL-PEI-CS_2 and Cu(II) [S2]. As presented in Fig. S4(c) and Table S2, all the fitted curves were separated into two linear segments and all the first lines did not pass through the origin. If the step is dominated by the intra-particle diffusion, the first linear segment should pass through the original point (I_1 = 0), otherwise the adsorption rate was considered to be affected with film diffusion and intra-particle diffusion or only film

diffusion ($I_1 \neq 0$) [S7]. As seen from Fig. S4(c) and Table S2, it was found that the I_1 values of the first portions were between -2.628 and 1.573 as the concentration ranged from 5 to 50 mg/L, which significantly kept away from the origin. In order to further ascertain the actually controlled step, Boyd's film-diffusion model was used for fitting experimental data before contact time of 90 min. When the lines of B_t versus t are linear and go through the original point, then the primary step is considered to be limited by intra-particle diffusion [S7]. When the lines are nonlinear or linear but do not go through the original point, and film diffusion controls the adsorption rate [S4]. Fig. S4D and Table S3 present the fitted curves and parameters of Boyd's model. The value of the intercepts for plots was from -0.465 to -0.045, all being far away from zero. From these results, the adsorption rate of Cu(II) over AL-PEI-CS_2 was proved to be determined by the film diffusion [S4].

The adsorption isothermal models of Langmuir and Freundlich were employed to fit the experimental data, and the results are presented in Fig. S4(e)-(f). As presented in Fig. S4(e), it can be concluded that Langmuir isothermal model described the experimental data well due to the R^2 was 0.9932, which was higher than that (0.9714) of Freundlich isothermal model. This result suggested that adsorption of Cu(II) onto AL-PEI-CS_2 was a monolayer process [S8]. Furthermore, the values of K_L and n were on a scale of 0 to 1 and 1 to 10, respectively, implying that the adsorption of Cu(II) on AL-PEI-CS_2 was a favorable process [S9, S10]. Fig. S4(e) also gives that the value of q_m for Cu(II) was calculated as 58 mg/g.

Table S1. Parameters of the Pseudo-first-order and Pseudo-second-order Kinetic Models for the Adsorption of Cu(II) onto AL-PEI-CS_2 at 25℃.

C_0 (mg/L)	$q_{e,exp}$ (mg/g)	Pseudo-first-order model			Pseudo-second-order model		
		$q_{e,cal}$ (mg/g)	K_1	R^2	$q_{e,cal}$ (mg/g)	K_2	R^2
5	4.679	4.705	0.016	0.9049	4.920	0.014	0.9894
10	9.545	4.477	0.019	0.8113	10.00	0.660	0.9955
15	14.34	22.86	0.020	0.9578	17.17	0.002	0.9574
20	19.06	29.11	0.021	0.9467	22.22	1.038	0.9761
30	28.24	42.65	0.018	0.9556	33.33	1.014	0.9512
50	48.14	73.60	0.017	0.8988	58.82	1.023	0.9801

Table S2. Parameters of the Intra-particle Diffusion Model for the Adsorption of Cu(II) onto AL-PEI-CS_2 at 25℃.

C_0 (mg/L)	Intra-particle diffusion model					
	K_{id1} (mg/g·min$^{1/2}$)	I_1 (mg/g)	R^2	K_{id2} (mg/g·min$^{1/2}$)	I_2 (mg/g)	R^2
5	0.467	0.325	0.8587	0.158	2.556	0.9627
10	1.019	1.432	0.8721	0.051	8.887	0.7642
15	1.602	1.573	0.9446	0.056	13.61	0.8440
20	1.896	0.009	0.9529	0.059	18.27	0.9256
30	2.740	-1.421	0.9797	0.832	17.26	0.8584
50	4.086	-2.628	0.9516	2.142	20.04	0.9349

Table S3. Parameters of the Boyd Kinetic Model for the Adsorption of Cu(II) onto AL-PEI-CS_2 at 25℃

Sorbate	C_0 (mg/L)	Boyd plot	
		Intercept	R^2
Cu(II)	5	-0.045	0.9278
	10	-0.465	0.9428
	15	-0.420	0.8816
	20	-0.364	0.9409
	30	-0.297	0.8451
	50	-0.088	0.9508

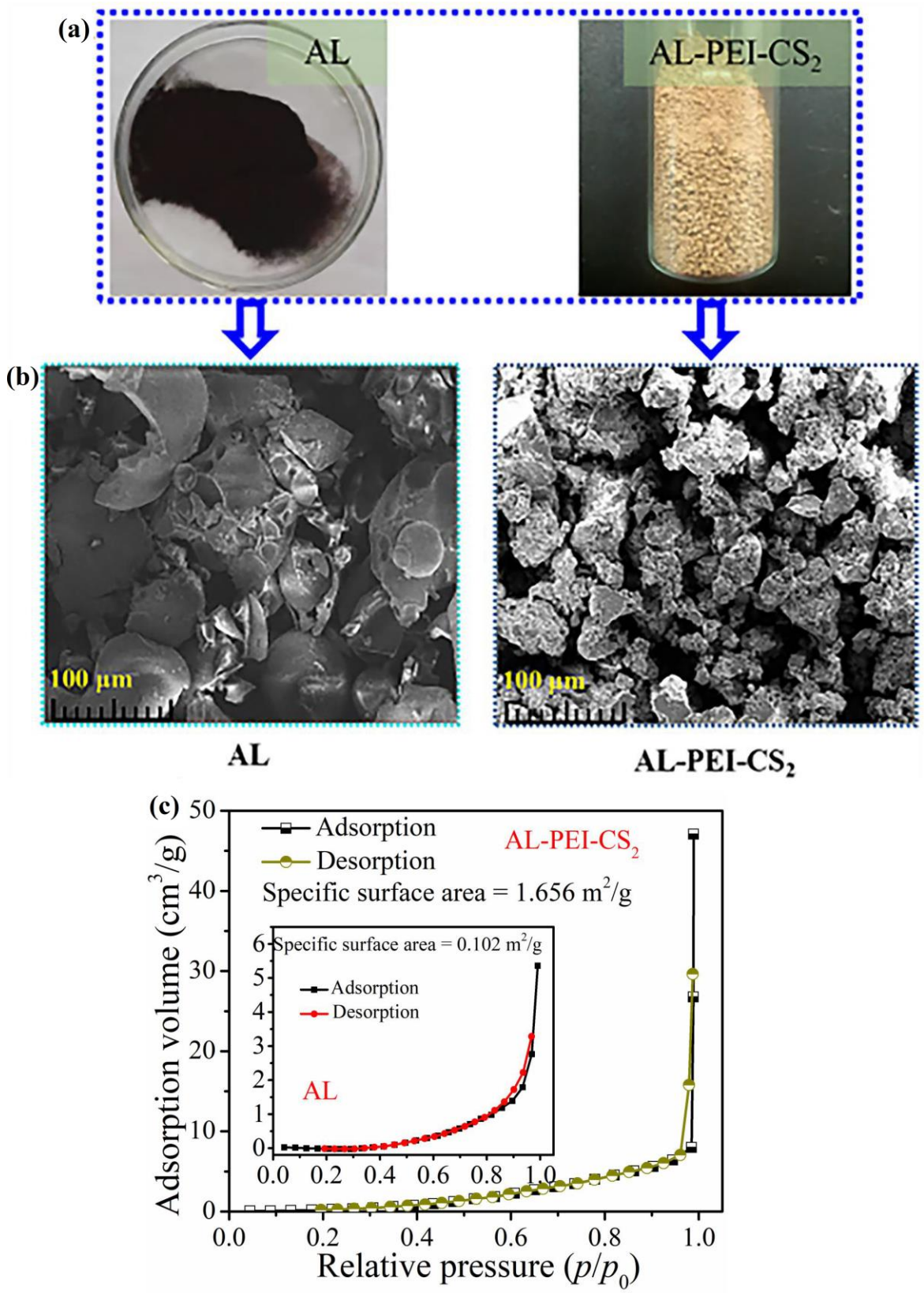

Fig. S1. Photographs (a) and SEM images (b) of AL and AL-PEI-CS_2; (c) N_2 adsorption-desorption isotherms measured at 77 K for AL and AL-PEI-CS_2.

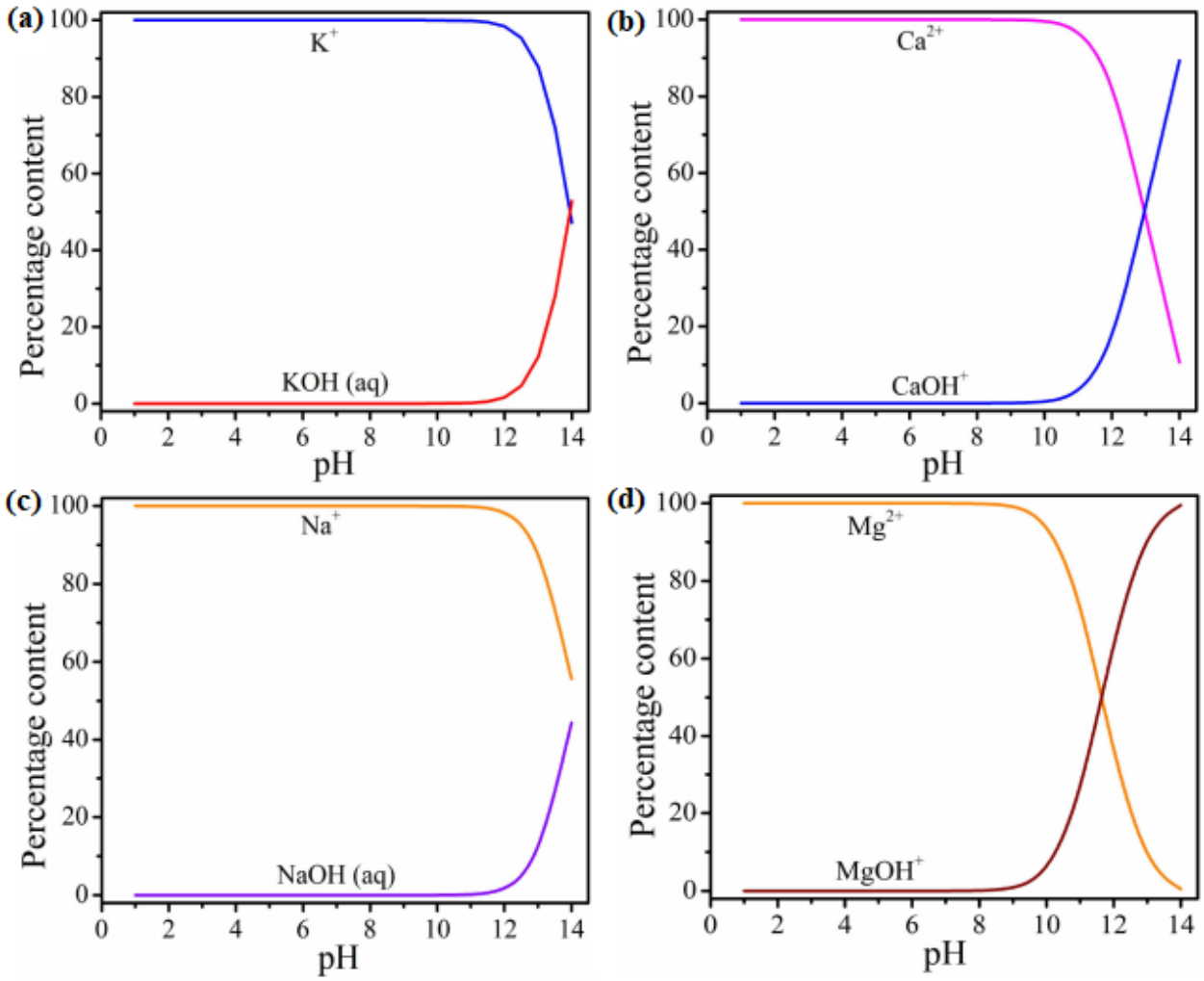

Fig. S2. Speciations of (a) potassium; (b) calcium; (c) sodium; and (d) magnesium at different pH values calculated with Visual MINEQL 3.0 software.

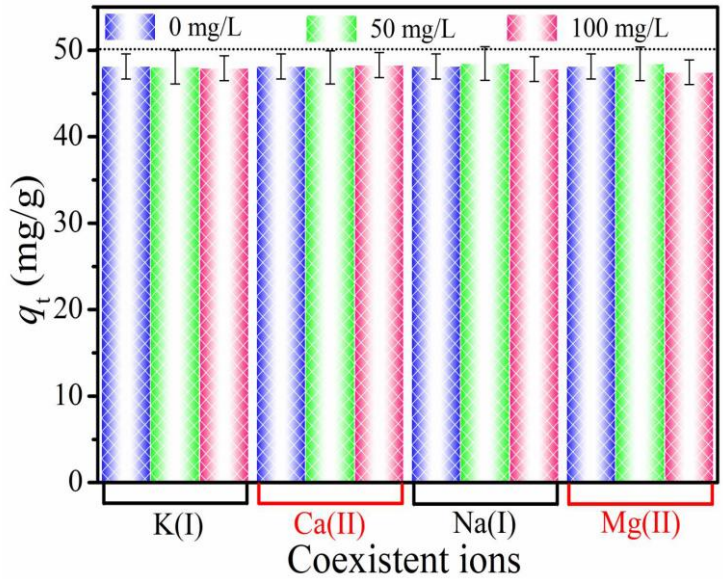

Fig. S3. Effect of the four cations on the adsorption of Cu(II) by AL-PEI-CS_2 at contact time of 180 min and C_0 of 50 mg/L Cu(II).

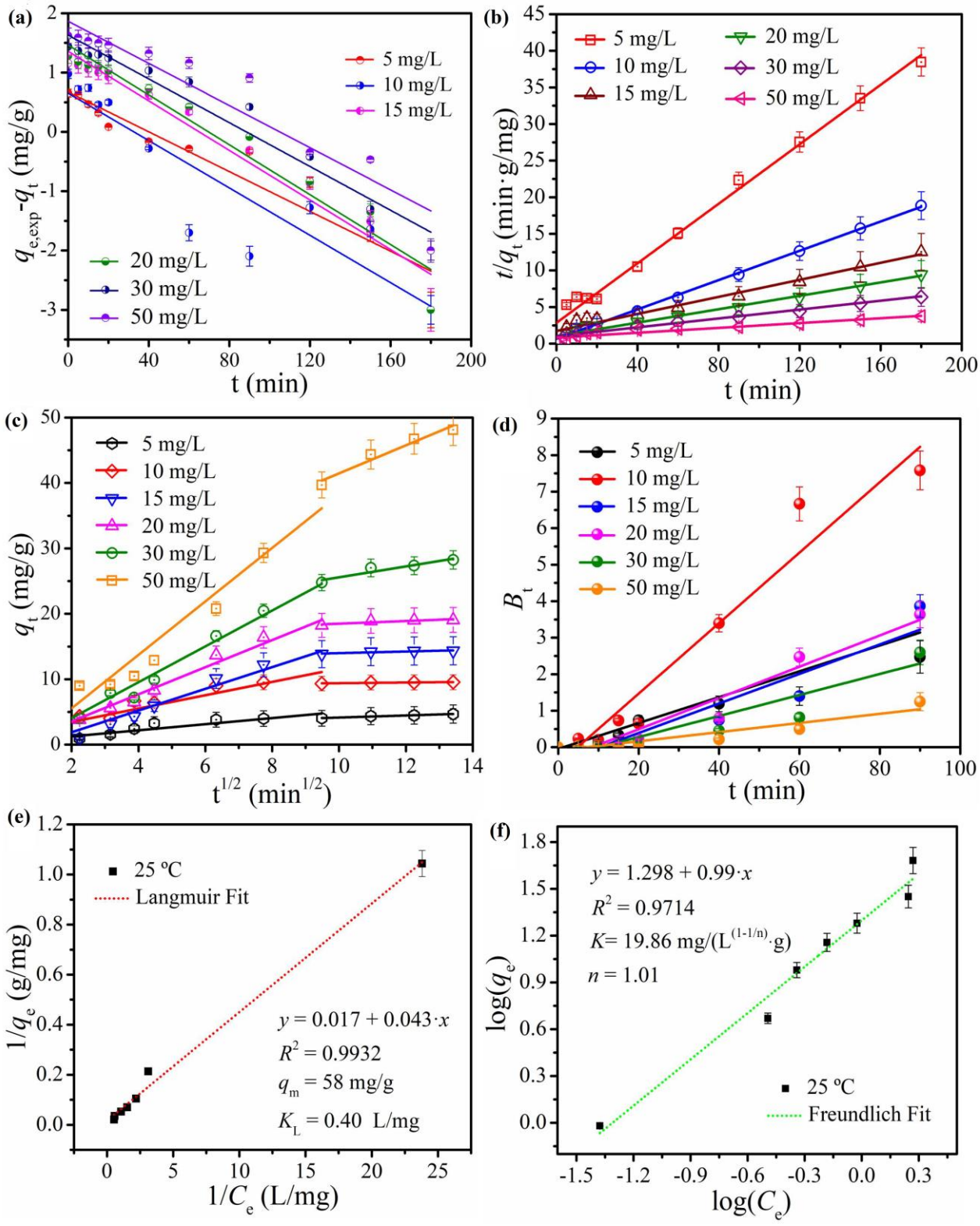

Fig. S4. Simulated plots of (a) the pseudo-first-order kinetic model; (b) the pseudo-second-order kinetic model; (c) the intra-particle diffusion model, (d) Boyd's film diffusion model; (e) Langmuir isothermal model; and (f) Freundlich isothermal model.

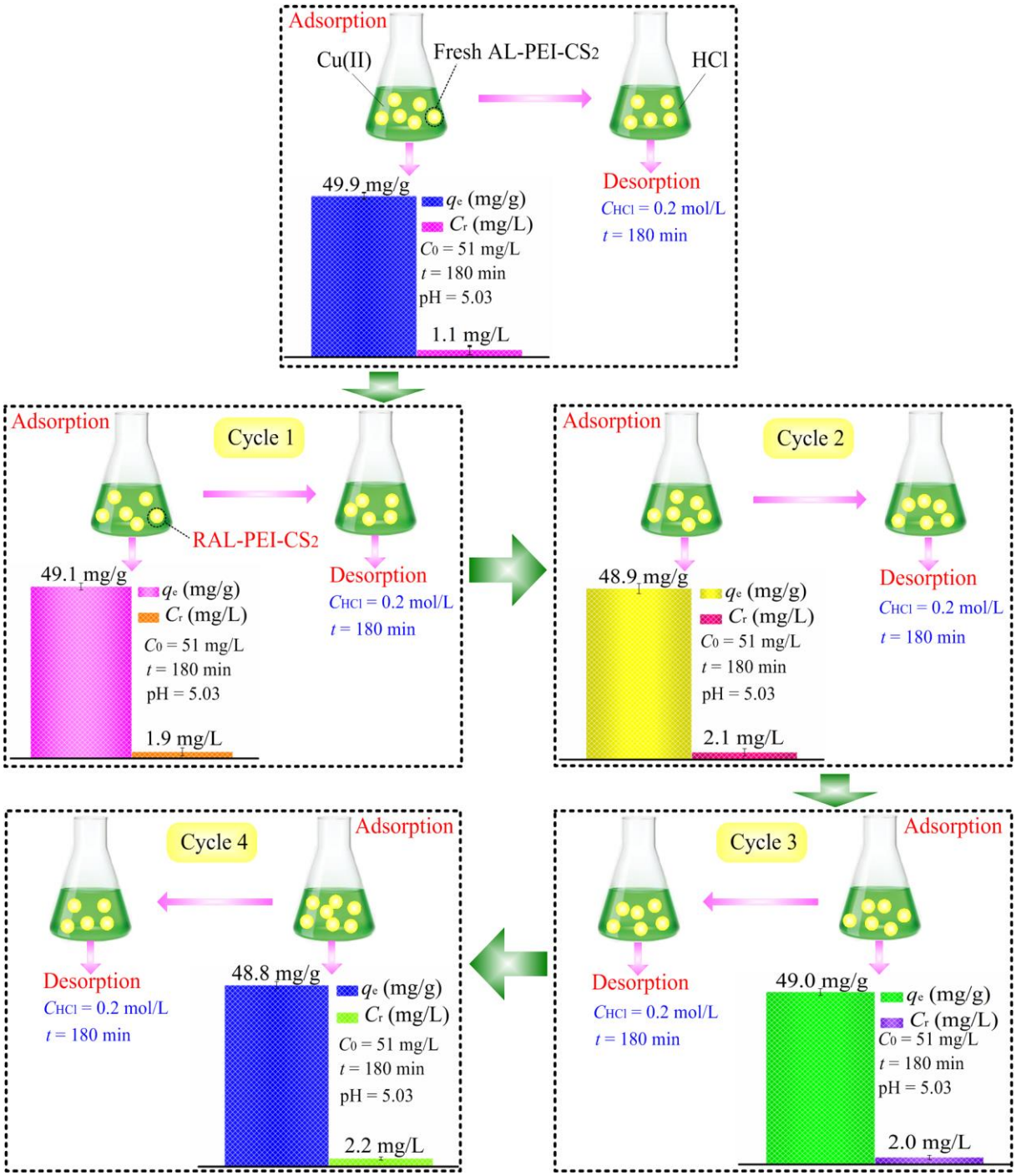

Fig. S5. Evaluation on the reusing ability for AL-PEI-CS_2 towards Cu(II).

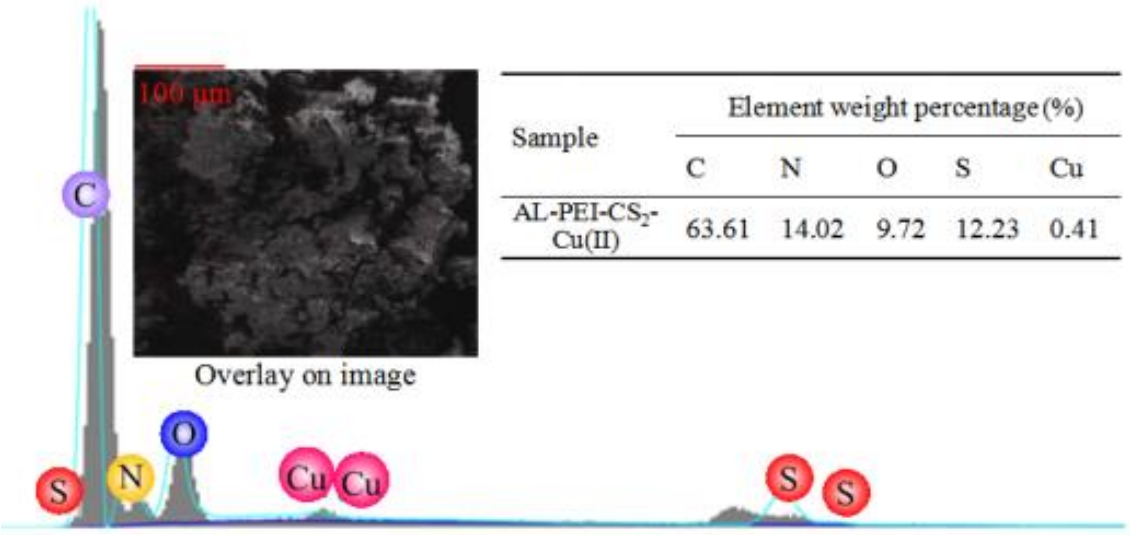

Sample	Element weight percentage (%)				
	C	N	O	S	Cu
AL-PEI-CS_2-Cu(II)	63.61	14.02	9.72	12.23	0.41

Fig. S6. SEM-EDS image for AL-PEI-CS_2-Cu(II) complexes.

References

S1. Ho, YS. Review of second-order models for adsorption systems. *J. Hazard. Mater.*. 2006;136:681-689.

S2. Ho YS, McKay G. Pseudo-second order model for sorption processes. *Process Biochem.* 1999;34:451-465.

S3. EI-Khaiary MI, Malash GF, Ho Y. On the use of linearized pseudo-second-order kinetic equations for modeling adsorption systems. *Desalinatio*n 2010;257:93-101.

S4. Tang B, Lin YW, Yu P, et al. Study of aniline/ε-caprolactam mixture adsorption from aqueous solution onto granular activated carbon: kinetics and equilibrium. *Chem. Eng. J.* 2012;187:69-78.

S5. Amin MT, Alazba AA, Shafiq M. Removal of copper and lead using banana biochar in batch adsorption systems: Isotherms and kinetic studies. *Arabian J. Sci. Eng*. 2018;43:5711-5722.

S6. Fan XL, Zou YF, Geng N, et al. Investigation on the adsorption and desorption behaviors of antibiotics by degradable MPs with or without UV ageing process. *J. Hazard. Mater*. 2021;401:123363.

S7. Tang Q, Wang KT, Yasseen M, et al. Synthesis of highly efficient porous inorganic polymer microsphere for the adsorptive removal of Pb^{2+} from wastewater. *J. Clean. Prod*. 2018;193:351-362.

S8. Langmuir, I. The adsorption of gases on plane surfaces of glass, mica and platinum. *J. Am. Chem. So*c. 1918;40:1361-1403.

S9. Ahmed MJ, Theydan SK. Microporous activated carbon from siris seed pods by microwave-induced KOH activation for metronidazole adsorption. *J. Anal. Appl. Pyrolysis* 2013;99:101-109.

S10. Freundlich, H. Ueber die adsorption in Loesungen. *J. Phys Chem*. 1906;57:385-470.